

**Master Advanced Lab Course
Universität Göttingen – Fakultät für Physik**

**Report on
the experiment KT.WZE**

W/Z experiment at the Tevatron

Name: Eric Bertok
Email: eric.bertok@stud.uni-goettingen.de
Conducted on 24th January 2018
Assistant: Dr. J. Veatch
Copy of document requested: yes no
Unterschrift:

Submission

Date: Signature of assistant:

Review

Date: Name of examiner:
Points: Signature:
Mark:

Contents

1. Introduction	1
2. Theory	1
2.1. Electroweak interaction	1
2.2. Matrix elements and Decay rates	1
2.3. Invariant and transverse mass	2
3. Experimental setup and methods	2
4. Analysis	3
4.1. Selection of $Z \rightarrow \mu\mu$ events	3
4.2. Cosmics	4
4.3. Zmass	4
4.4. Reconstructing and selecting W events	4
4.5. Determination of efficiencies	8
4.6. Determination of the $BR(W \rightarrow \mu\nu)$	8
5. Discussion	8
A. Z boson additional plots	11

1. Introduction

In goal of this experiment is the determination the of the branching ratio of the W boson $\text{BR}(W \rightarrow \mu\nu)$. First, W and Z bosons are reconstructed using data provided by the Tevatron collider at Fermilab. By comparing with Monte Carlo simulations, selection parameters are obtained, which allow for clean cuts for filtering out background events (jets and cosmic source). The mass and the transverse mass is then determined for the Z and W boson respectively. Finally the branching ratio is calculated from the number of selected events, the trigger efficiencies, as well as the reconstruction efficiencies.

2. Theory

2.1. Electroweak interaction

The GWS theory (Glashow, Weinberg, Salam) is the unified description of both the electromagnetic force mediated by the photon and the weak interaction mediated by the massive W^+ , W^- and the neutral neutral Z boson. It was confirmed experimentally in the 1970s [4]. The gauge bosons are introduced by means of a local $SU(2)_L$ gauge symmetry in a weak isospin space. The weak isospin doublets are formed by fermions differing by one unit of charge [5, p.;416]. By also replacing the $U(1)$ symmetry by a new $U(1)_Y$ symmetry with the “hypercharge” Y , the neutral Z boson can be identified by a linear combination of the neutral $W^{(3)}$ boson and the B boson coupling to the hypercharge. More details can be found in [5, p. 418ff]. Being a charged boson, the W bosons couple to fermions differing by one unit of charge. Furthermore it maximally violates parity as it only couples to left-handed particles and right-handed antiparticles. The vertex factor is given by [5, p.;409]

$$-i\frac{g_W}{\sqrt{2}}\frac{1}{2}\gamma^\mu(1-\gamma^5), \quad (2.1)$$

where g_W is the weak coupling constant and γ^μ are the gamma matrices. The Z boson however, couples to any pair of identical fermions, albeit coupling more strongly to left handed ones. This becomes apparent in the form of the vertex factor: [5, p. 432]

$$-i\frac{1}{2}g_Z\gamma^\mu(c_V - c_A\gamma^5), \quad (2.2)$$

with the vector and axial vector couplings c_V and c_A .

2.2. Matrix elements and Decay rates

The matrix elements for the electroweak interaction can be calculated with the appropriate Feynman rules. After averaging over the three possible polarizations, the spin-averaged matrix element squares is obtained for both the W and the Z boson decaying to a lepton and its neutrino or a lepton- anti-lepton pair, respectively [5, p.;242,411]:

$$\langle|\mathcal{M}_W^2|\rangle = \frac{1}{3}g_W^2m_W^2 \quad (2.3)$$

$$\langle|\mathcal{M}_Z^2|\rangle = \frac{1}{3}(c_V^2 + c_A^2)g_Z^2m_Z^2. \quad (2.4)$$

These can be inserted into the decay rate formula: [5, p. 411]

$$\Gamma = \frac{p^*}{32\pi^2m^2} \int \langle|\mathcal{M}^2|\rangle d\Omega = \frac{p^*}{8\pi m^2} \langle|\mathcal{M}^2|\rangle, \quad (2.5)$$

where m is the mass of the boson and p^* is the momentum of the lepton in the center of mass frame. One can argue that $p^* = m_Z/2$, as the decay happens in the centre of mass frame of the decaying particle. Therefore the decay rate is

$$\Gamma(W^- \rightarrow e^-\bar{\nu}_e) = \frac{g_W^2m_W}{48\pi}. \quad (2.6)$$

$$\Gamma(Z \rightarrow e^-e^+) = \frac{g_Z^2m_Z}{48\pi}(c_V^2 + c_A^2). \quad (2.7)$$

Lepton universality tells us that this is the same for all three leptonic channels when neglecting masses. For hadronic processes, the CKM matrix has to be considered, while excluding the top quark, as it is too massive. For the W boson, one obtains for the decay width [cite]

$$\Gamma_W = (3 + 6\kappa)\Gamma(W^- \rightarrow e^-\bar{\nu}_e) \approx 9.2 \frac{g_W^2 m_W}{48\pi} = 2.1 \text{ GeV}. \quad (2.8)$$

$\kappa \approx 1.038$ is a correction factor that accounts for second order QCD processes. Similarly, for the Z boson, one obtains

$$\Gamma_Z \approx 2.5 \text{ GeV}. \quad (2.9)$$

The branching ratios for the muon channel are therefore

$$BR(W \rightarrow \mu\bar{\nu}_\mu) = 10.8\%, \quad (2.10)$$

$$BR(Z \rightarrow \mu^+\mu^-) = 3.5\%. \quad (2.11)$$

2.3. Invariant and transverse mass

For the Z boson one can calculate the functional form of the invariant mass peak by taking into account its finite lifetime. The cross section for a $q\bar{q} \rightarrow \mu^+\mu^-$ event is proportional to [cite]

$$\sigma \propto |\mathcal{M}|^2 \propto \left| \frac{1}{q^2 - m_Z^2 + im_Z\Gamma_Z} \right|^2 = \frac{1}{(q^2 - m_Z^2)^2 + m_Z^2\Gamma_Z^2}, \quad (2.12)$$

which is a Breit-Wigner curve. q is the invariant mass of both muons. As both can be detected in such an event, the Breit-Wigner-curve can be fitted directly to the selected data to obtain the mass of the Z boson. For the W boson, things are more complicated. Due to the W events only having one muon, the undetectable neutrino has to be reconstructed from the missing momentum. For a hadronic collider such as the tevatron, the total centre of mass energy cannot be known on an event to event basis [cite] due to the composite nature of the hadrons. More specifically, the z -momentum of the interacting partons are unknown, making the invariant mass reconstruction impossible. However, one can define the transverse mass M_T , which can be calculated from the reconstructed transverse momentum of the neutrino \mathbf{p}_T^ν . First, the missing transverse energy MET is determined as

$$MET \approx |\mathbf{p}_T^\nu| = |-\mathbf{p}_T^\mu - \mathbf{u}_T|, \quad (2.13)$$

where \mathbf{u}_T is the transverse momentum of the hadrons [cite]. The transverse mass is then defined as

$$M_T = \sqrt{(MET + \mathbf{p}_T^\mu)^2 - (MET_x + p_x^\mu)^2 - (MET_y + p_y^\mu)^2}. \quad (2.14)$$

This quantity is lorantz invariant but does not peak at m_Z . However, the W mass can be read off from the position of the dropoff, as the longitudinal component of the invariant mass is then close to zero [cite].

3. Experimental setup and methods

For this experiment, 2 types of data have been provided: The first is a subset of real data from the DØ detector at Fermilab near Chicago. The second are two sets of simulated monte-carlo W and Z events generated by PYTHIA [cite].

At the DØdetector, muons are identified both in the muon detector and the tracking system. Whereas the tracking system directly surrounds the interaction point and allows for gauging the muon's momentum and direction precisely, the outer muon detector is mostly used to match the track in the tracking system. This is possible because muons are the only particles capable of reaching the muon detector, due to a combination of their relatively long lifetime and small calorimeter energy deposition. [cite?] For more details on the DØ detector see [3]. As the sheer amount of data from the collider is too much to analyse and save, both software and hardware triggers are used to decide, whether an event is worth investigating. The data that is provided is pre-filtered for at least one muon in every event that has a transverse momentum of at least 15 GeV/c. [??? zusätzlicher trigger] The monte-carlo data has been reconstructed, such that the events look like real data. Therefore the monte-carlo serves a benchmark for the analysis of the real data. To obtain invariant mass peaks for the Z - aswell as the transverse mass peak for the W

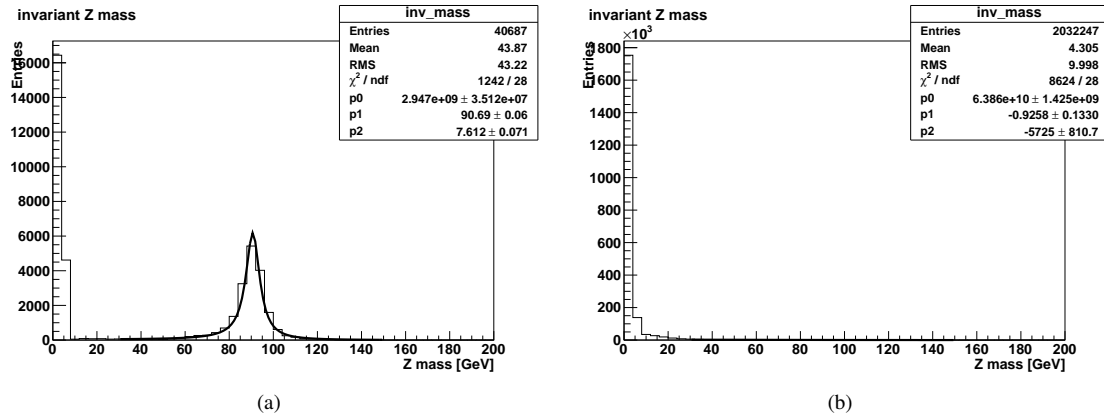


Figure 1: Z mass plotted for both monte-carlo (left) and real data (right) without any cuts. One can clearly see the expected mass peak at the monte carlo case, aswell as a leage number of events with very low mass, while in the real data plot, no mass peak is visible yet. For the monte-carlo case, a χ^2 fit is performed with the Breit-Wigner curve.

boson, the right events have to be selected out of the 3 million events provided. This happens by first fixing a set of object level cuts, which define what is counted as a muon. These cuts are the same for both W - and Z boson analysis. Secondly, a range of object level cuts have to be performed to single out the right events for Z and W production respectively. These have to be physically motivated by keeping in mind what is expected for the muons in a W or Z decay and should also be compared to the monte-carlo simulation. By first comparing various muon parameters for the simulated data and the uncut experimental data, one can define appropriate cuts in these parameters that cut out most events not present in the simulation while also keeping events that do resemble the simulation mostly intact. Finally the real data is plotted with these cuts performed and compared with the simulated results. This process is repeated until a satisfactory isolation of Z or W events has been produced. All of the analysis is done with ROOT.

4. Analysis

4.1. Selection of $Z \rightarrow \mu\mu$ events

The Z boson mass distribution for the simulated monte-carlo data is shown in fig. 1(a). One can clearly see the mass peak of the Z boson. A large number of events, however, is also situated at the beginning of the mass spectrum. A fit performed by root with the function 4.1

$$\sigma \propto \frac{1}{(q^2 - m_Z^2)^2 + m_Z^2 \Gamma_Z^2} \quad (4.1)$$

is performed, with the parameters p_0 as a constant proportionality factor, p_1 being m_Z and p_2 being the decay width Γ . The results are summarized together with all other fits in table 2. Apart from the large number of events at low mass, this clearly resembles the expected Z mass peak. In fig. 1(b), the uncut real data is plotted. From the 2 million events, almost all of them give a very small Z mass and the peak is not visible. Note that the trigger "TRIG_MUW_W_L2M3_TRK10" [2] is still included in the uncut case. Additional object level cuts are performed, which are summarized in table 1. These are identical for both Z and W boson analysis as they will effectively cancel out when calculating the efficiencies. The accepted and rejected events for both Z monte-carlo and real data are shown in section A (figs. 8 to 10). To further separate background events, event level cuts are performed. Firstly, events where only one muon are detected are rejected, as in a Z decay, two muons are expected. Secondly, both muons should have different charge due to conservation of charge. Two muons with same charge indicate either two seperate processes both creating a positively / negatively charged muon or a cosmic event in which one cosmic muon crosses both detectors.

parameter	condition	description
p_{T_1}	> 20	transverse momentum of the first muon in the central tracker
p_{T_2}	> 15	transverse momentum of the second muon in the central tracker
$\chi^2_{1/2}$	< 2	Chi squared per d.o.f. for the track fit
$E_{\text{halo}_{1/2}}$	< 1.5	transverse calorimeter energy in an annulus of $0.1 < R < 0.4$ around the muon

Table 1: Additional object level cuts for the muons for both Z and W analysis.

Data set	m_Z [GeV]	Γ_Z [GeV]
Z monte-carlo uncut	90.69 ± 0.06	7.612 ± 0.071
Z monte-carlo cut	91.64 ± 0.03	4.448 ± 0.088
real data cut	90.19 ± 0.15	11.85 ± 0.20
Theoretical result [1]	91.1876 ± 0.0021	2.4952 ± 0.0023

Table 2: Summary of reconstructed Z mass m_Z and decay width Γ_Z for both cut and uncut simulated data ,as well as real data obtained from the Breit-Wigner fit.

4.2. Cosmics

The cosmic-ray background stems from high energy cosmic particles entering the earth's atmosphere, where they decay into jets of particles. Muons are also created this way. Because of time dilation, they can reach the earth's surface before they decay, leading to the cosmic background in the detector [cite]. In order to identify cosmic events, both timing and angular separation are taken into account. First, it is expected that timing differences from muons originating from Z decays have a negligible time difference at both muon detectors, since the Z boson can be treated as stationary in the lab frame. Cosmic muons, however, should be detected at one side of the detector first and at a later time on the other side, since they need to travel the distance of the detector first. The timing difference for Z monte-carlo and real data is plotted in fig. 2. A maximal time difference of $\Delta t = 10$ ns was chosen as cut condition. However, also the simulated data shows two peaks at around 100 ns. Next, a two-dimensional histogram is plotted with the angular separation $\Delta\eta$ and $\Delta\phi$ as parameters. η is the pseudorapidity of the track and gives a measure of the tilt from the beam axis, while ϕ is the angle around the beam axis. The result is shown for the simulation and real data in fig. 3. Note that so far, no angular cuts have been performed at all. Still, with the cuts given above, there is a clear preference for $\Delta\phi = \pi$ for both simulation and real data. This is desired, as this means that the Z boson upon its decay is quasi-stationary and therefore both muons produced in the decay travel in opposite directions, as expected from momentum conservation. Therefore, a decision was made not to perform any more cuts containing angular information. As will be seen below, the cuts performed thus-far give a very satisfactory result for the reconstructed Z mass peak. The reason for this will be discussed in section 5.

4.3. Zmass

The invariant Z mass can be calculated directly with ROOT with the TLorentz-vector class. In theory, the muon mass is not needed for a reconstruction of the Z events, as $E \approx p$ holds for the ultrarelativistic case, which is fulfilled for the muons in question. Finally, with the cuts performed, the Z mass is plotted in figs. 4(a) and 4(b) for both Z monte-carlo and real data. One now clearly observes the expected mass peak also in the real data. The rejected events mostly consist of low- Z -mass events and cut out very little from the actual mass peak, which is especially apparent in the simulated data. Again, a fit is performed for the Breit-Wigner curve eq. (4.1). The results are summarized in table 2.

4.4. Reconstructing and selecting W events

As outlined in section 2, the invariant W mass cannot be directly reconstructed. This is due to the neutrino in the decay products, which is not detectable. More specifically, the longitudinal momentum component of the W is outside of reach because of the composite structure of the colliding protons. As a result, the total centre of mass energy is unknown on an event by event basis. As the missing neutrino momentum can only be inferred from the missing energy, this means that the z-component of the energy is not detectable. It is therefore the goal to define selections that reconstruct the transverse mass eq. (2.14). The uncut transverse mass of the W monte-carlo simulation is shown in fig. 5(a). As expected, it does not peak at the W mass, however the location of the dropoff

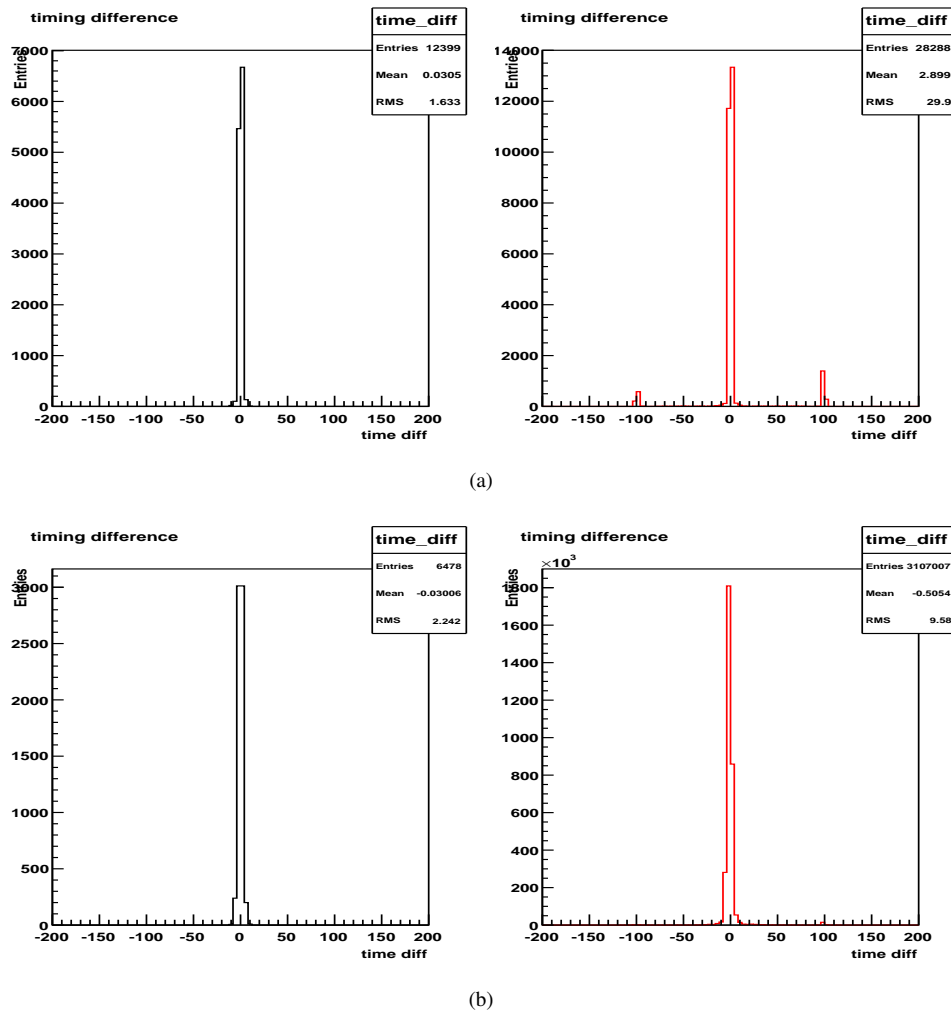


Figure 2: Timing difference between the first and second muon detection for the Z monte-carlo (a) and the real data (b) in ns.

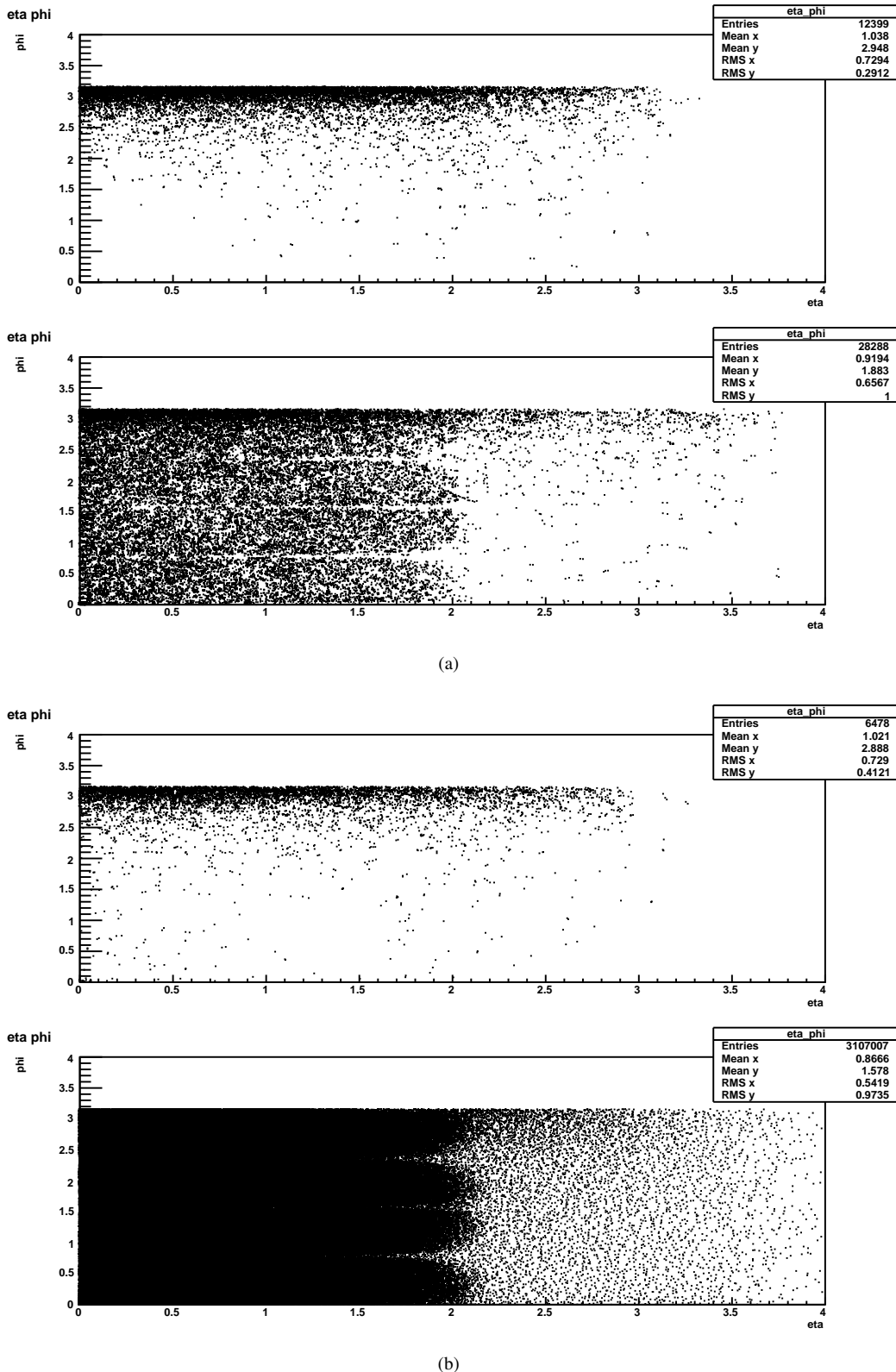


Figure 3: Two-dimensional histogram of the difference between pseudorapidity $\Delta\eta$ and difference between azimuthal angle $\Delta\phi$ of both muons for simulated (a) and real data (b). The upper plots are the accepted events, the lower plots are the rejected events. With the cuts detailed above, there is a clear preference of $\Delta\phi = \pi$ in both simulation and real data. Also, lower pseudorapidity difference $\Delta\eta$ is more common. For the uncut case, both simulation and real data shows additional structure at non- 2π azimuthal difference. Note that no angular cuts have been performed in either case.

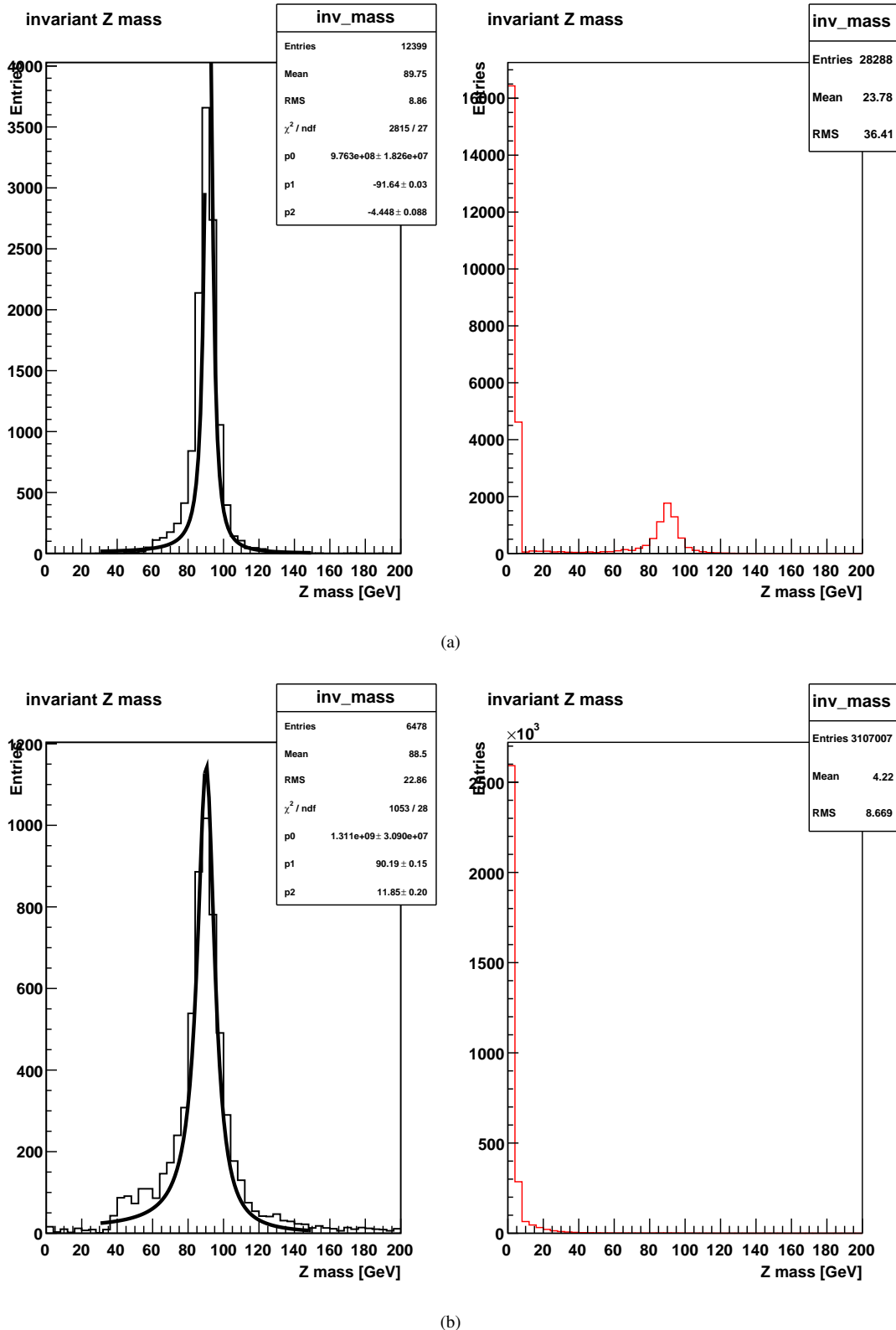


Figure 4: Reconstructed Z mass for the simulated (a) and real data (b). On the left in black, the accepted events are plotted, on the right the rejected ones. Apart from a small trail on the higher mass spectrum, both peaks look qualitatively the same. The cuts mostly got rid of the low Z -mass events, as can be seen by comparison of simulation and data. A χ^2 fit for the Breit-Wigner curve is performed on the accepted events.

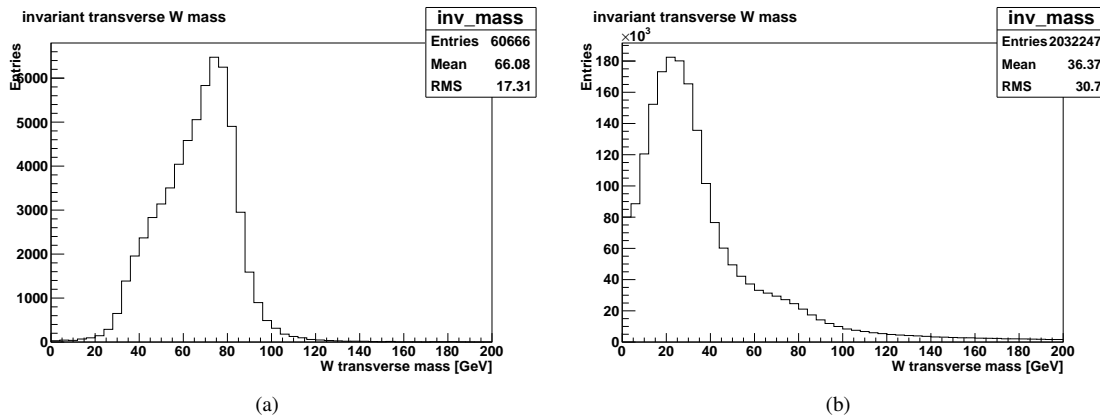


Figure 5: (a): Uncut transverse mass distribution of the W monte-carlo simulation. The dropoff occurs at around 80 GeV, which is consistent with the literature value. (b): Uncut transverse mass distribution of the real data. The data is dominated by low-transverse mass events.

fits the theoretical W mass result of $m_W = 80.385 \pm 0.015$ GeV [1]. The uncut real data plot fig. 5(b) does not have this feature: the background consisting mostly of cosmics dominates in low transverse mass regions [??]. In addition to the object level cuts from table 1, different event level cuts are performed:

- $20 \text{ GeV} < \text{MET} < 60 \text{ GeV}$
- only one muon passes the trigger (since one muon and one neutrino is expected)

These two additional conditions are enough for a satisfactory reconstruction. Cosmics are automatically filtered out, since they almost always correspond to two muons detected at different times but only one muon is required with the selections. The condition for the missing transverse energy was mostly found by trial and error and by comparing different parameters of the simulated and the real data. The resulting MET cuts are shown in figs. 6(a) and 6(b). With the cuts in place, both accepted distributions look similar. Finally, the reconstructed transverse mass of the W boson can be calculated from eq. (2.13). It has to be kept in mind, that the muon is a minimal ionising particle and therefore does not deposit its energy into the calorimeter. Thus, when calculating the total missing transverse energy, the muon momentum has to be added which in the relativistic case is $E_{T\mu} = p_{T\mu}$. The formula for the transverse mass therefore reads

$$M_T = \sqrt{(E_{\text{cal}} + 2p_{T\mu})^2 - (E_{\text{cal},x})^2 - (E_{\text{cal},y})^2}. \quad (4.2)$$

[??]

The resulting transverse energy is plotted in fig. 7(b). With cuts in place, the experimental data now also shows the expected dropoff at around 80 GeV. Only around one percent of experimental events passed the selection criteria. Mostly low m_T background was rejected. Still, also about one third of monte-carlo events were rejected, which might indicate an overselection [??].

4.5. Determination of efficiencies

4.6. Determination of the $BR(W \rightarrow \mu\nu)$

5. Discussion

References

- [1] Particle Data Group: gauge boson summary sheet. <http://pdg.lbl.gov/2017/tables/rpp2017-sum-gauge-higgs-bosons.pdf>. – Zugriff:2018-01-31
- [2] Praktikumshandbuch. master-fp.physik.uni-goettingen.de. – Zugriff:2018-01-31

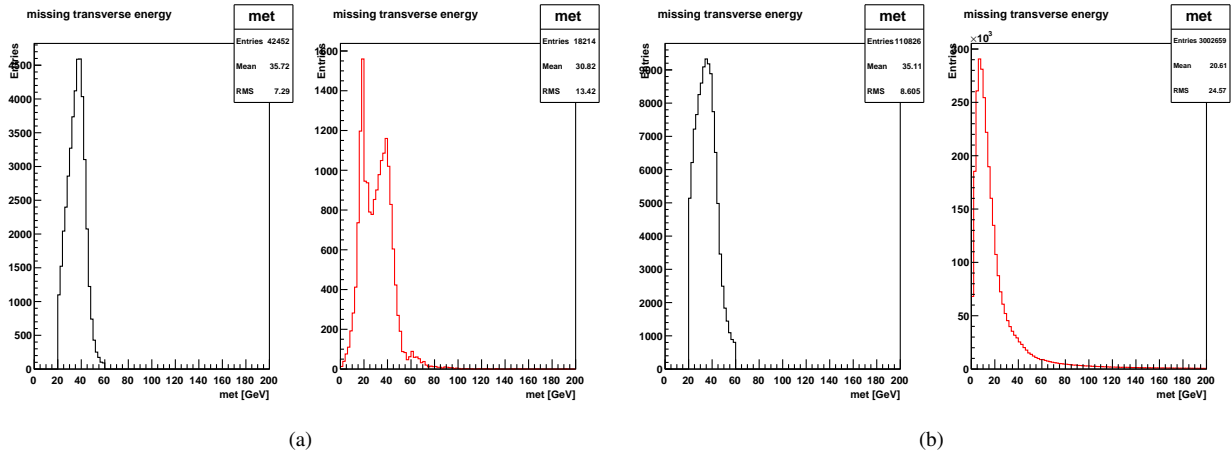


Figure 6: Missing transverse energy distribution for both simulation (a) and real data (b). Shown in black are the accepted events and in red are the rejected ones. With the cuts performed both accepted distributions look close to each other.

- [3] *Public web page of the DØ experiment.* <http://www-d0.fnal.gov/public/index.html>. – Zugriff:2018-01-31
- [4] *Wikipedia: electroweak interaction.* https://de.wikipedia.org/wiki/Elektronschwache_Wechselwirkung. – Zugriff:2018-01-31
- [5] THOMSON, Mark: *Modern Particle Physics*. Cambridge University Press, 2013

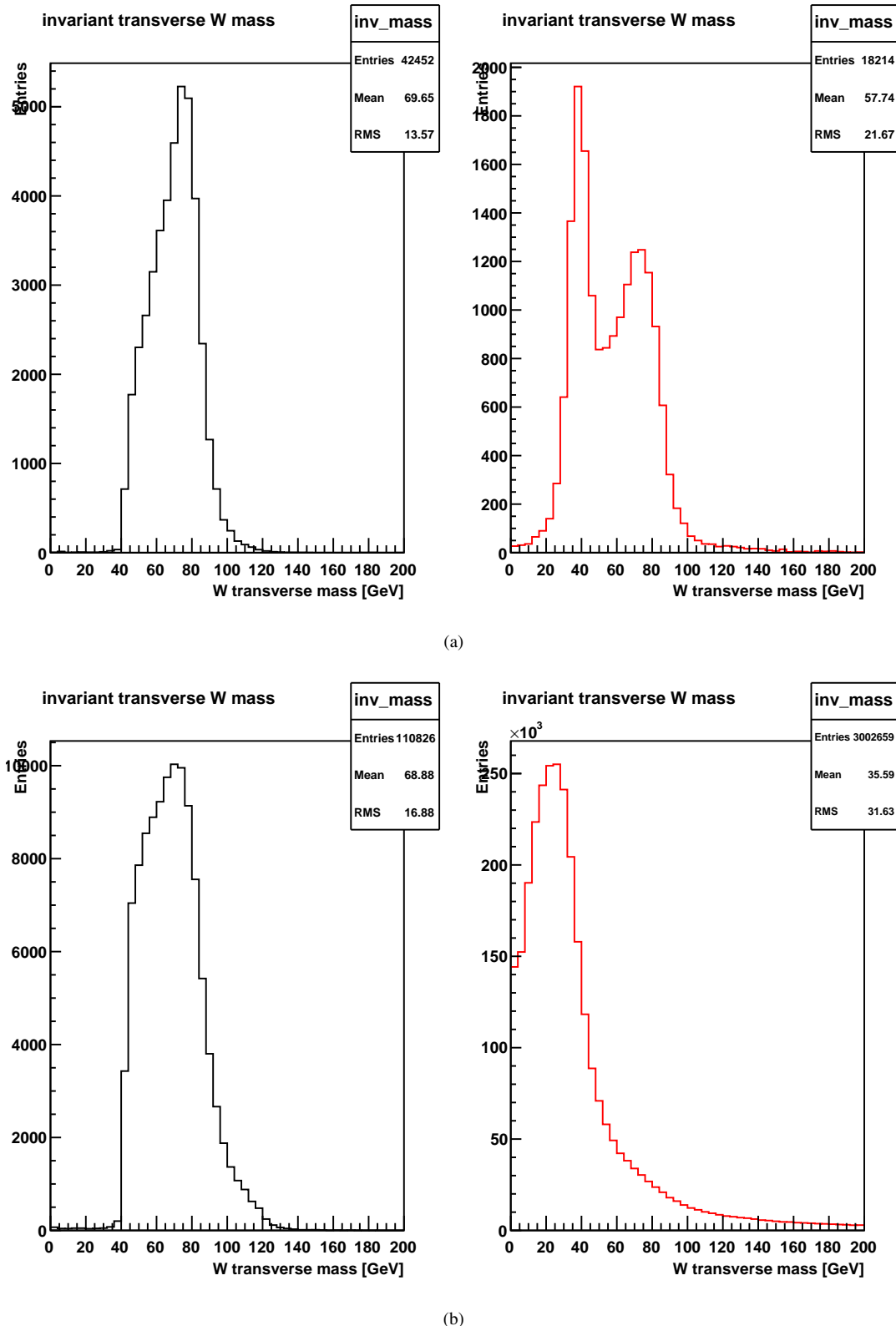


Figure 7: Reconstructed transverse W mass for the simulated data with cuts (a) and for the cut real data (b). In black: selected events. In red: rejected events. The selection mostly rejected low m_T background [consisting of ???]. The expected dropoff at around 80 GeV is now visible for the experimental data. However, also about one third of monte carlo events were rejected by our selection.

A. Z boson additional plots

A Z BOSON ADDITIONAL PLOTS

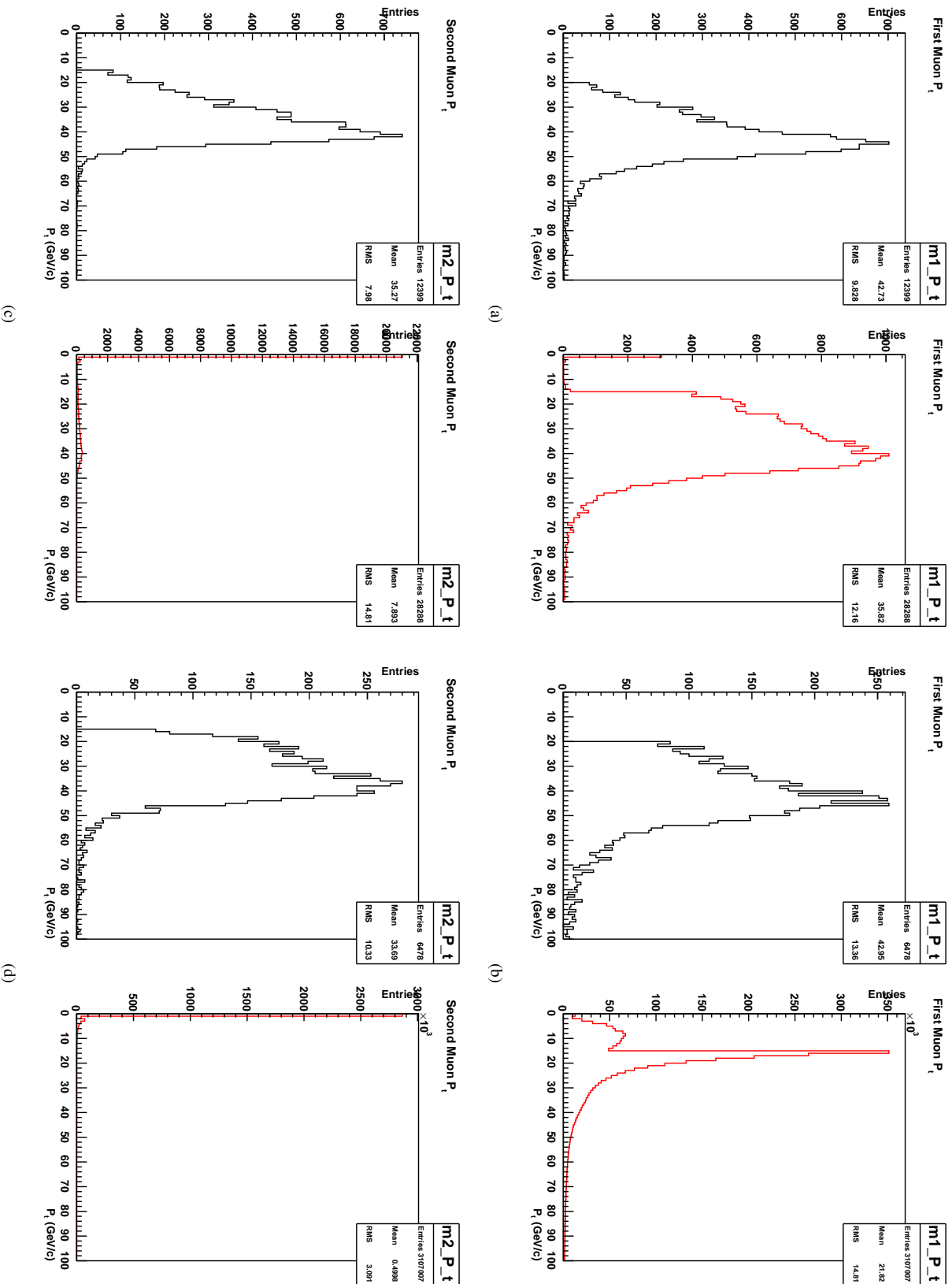


Figure 8: p_T for accepted (black) and rejected (red) events for (a,c): the Z monte-carlo data (b,d): the real data.

A Z BOSON ADDITIONAL PLOTS

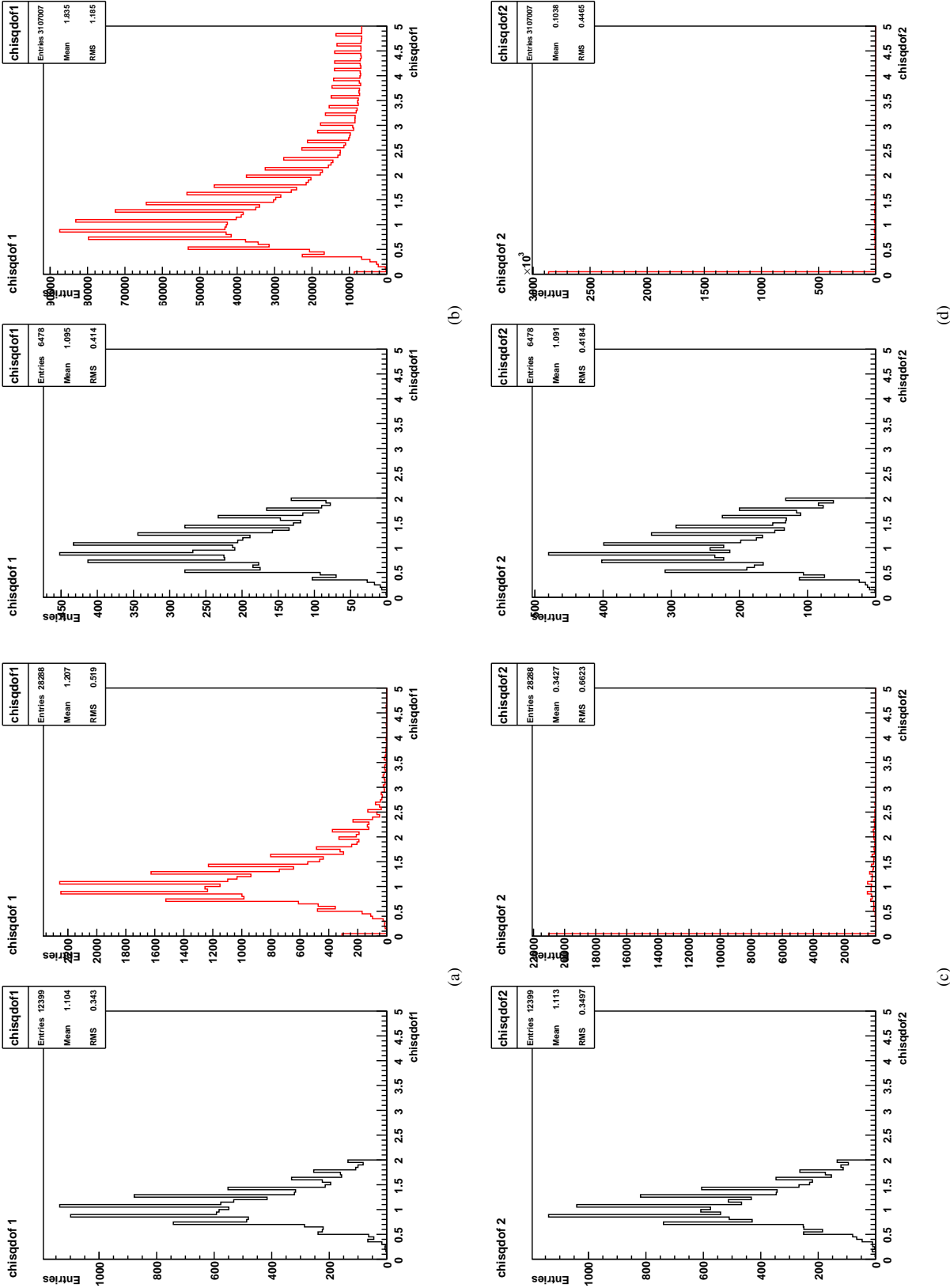


Figure 9: χ^2 for accepted (black) and rejected (red) events for (a,c); the Z monte-carlo data (b,d); the real data.

A Z BOSON ADDITIONAL PLOTS

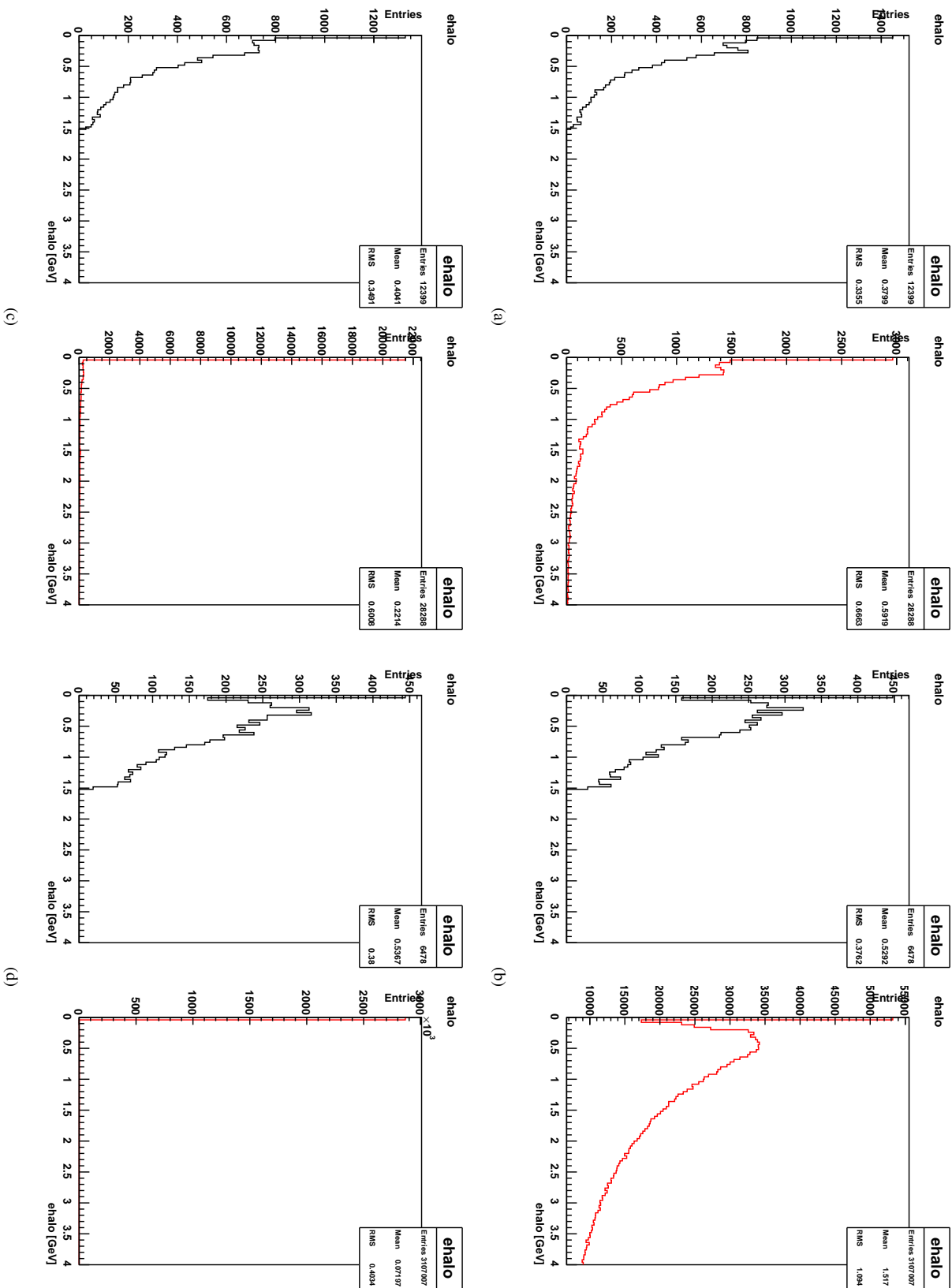


Figure 10: E_{halo} for accepted (black) and rejected (red) events for (a,c): the Z monte-carlo data (b,d): the real data.